P1.6 EVALUATING EFFECTIVENESS OF THE FAA'S CIT AVOIDANCE GUIDELINES

John K. Williams*, Jamie K. Wolff, Andrew Cotter, and Robert D. Sharman
National Center for Atmospheric Research, Boulder, Colorado

1. INTRODUCTION

The Federal Aviation Administration's thunderstorm avoidance guidelines include restrictions on flight in and around thunderstorms whose aim is to reduce the number and severity of hazardous encounters with convectively-induced turbulence (CIT). When convective activity is widespread, these restrictions can have a significant impact on the national airspace system, causing delays, cancellations, and additional fuel expense for airlines as aircraft are diverted around thunderstorms. For this reason, unnecessarily restrictive guidelines may be inconvenient and costly for both airlines and passengers. On the other hand, guidelines that do not adequately address the hazard posed by CIT may compromise aviation safety. Therefore, under direction and funding from the FAA's Aviation Weather Research Program, a study is underway to determine whether the current CIT avoidance guidelines are supported by the available data, and whether refinements or additions may be appropriate.

This paper presents preliminary statistical analyses and case studies that exploit newly available quantitative turbulence data produced by the FAA's automated *in situ* turbulence reporting system, which is currently operational on United Airlines B-737 and B-757 aircraft. Data from several thousand summertime flights were used to identify turbulence encounters near thunderstorms, as identified by the National Convective Weather Detection product and by radar reflectivity mosaic data produced by the summer, 2005, real-time demonstration of the NCAR Turbulence Detection Algorithm.

2. THE FAA'S CIT AVOIDANCE GUIDELINES

Studies of historical data have shown that over 60% of turbulence-related aviation accidents are due to convectively-induced turbulence (CIT), many of them in the clear air outside of thunderstorms (Cornman and Carmichael 1993; see also Kaplan et al. 2005). CIT is among several thunderstorm-associated hazards cited in FAA Advisory Circular 00-24, "Thunderstorms", dated 20 January 1983 (available on the Internet at the URL www.airweb.faa.gov/Regulatory_and_Guidance_Library/rgAdvisoryCircular.nsf/) and in the FAA Aeronautical Information Manual (AIM), section 7-1-30, "Thunderstorm Flying" (available from www.faa.gov/atpubs/AIM/). Other thunderstorm hazards include tornadoes, icing, low ceiling and visibility, lightning, and engine water ingestion. However, out-of-cloud CIT is unique in that it may occur well outside a thunderstorm and is essentially invisible to a pilot. While the Graphical Turbulence Guidance (GTG) system (Sharman et al. 2002 and 2006) provides clear-air turbulence forecasts that may, in certain situations, capture some of the environmental conditions involved in CIT generation and propagation, there is currently no operational system that provides airline dispatchers, air traffic controllers, or pilots with timely, reliable information about the dynamic threat from CIT. The FAA's thunderstorm avoidance guidelines, along with other rules of thumb gathered through experience, are currently their best source of information.

The FAA thunderstorm avoidance guidelines relevant to CIT, as stated in both AC 00-24 and the AIM, include the following:

- *Don't attempt to fly under a thunderstorm even if you can see through to the other side. Turbulence and wind shear under the storm could be disastrous.*
- *Do avoid by at least 20 miles any thunderstorm identified as severe or giving an intense radar echo. This is especially true under the anvil of a large cumulonimbus.*
- *Do clear the top of a known or suspected severe thunderstorm by at least 1,000 feet altitude for each 10 knots of wind speed at the cloud top.*
- *Do circumnavigate the entire area if the area has 6/10 thunderstorm coverage.*
- *Do regard as extremely hazardous any thunderstorm with tops 35,000 feet or higher whether the top is visually sighted or determined by radar.*

The present study seeks to address the first three of these guidelines by examining whether there is a statistical correlation between proximity to convection, either horizontal or vertical, with the incidence of turbulence. In addition, several case studies are presented to illustrate what further analysis may be possible.

3. STATISTICAL COMPARISONS

In the initial study presented below, analyses of aircraft-measured turbulence intensity values as a function of horizontal and vertical distance to convection are performed. The turbulence intensity values are supplied by the FAA's operational *in situ* turbulence reporting system (Cornman et al. 1995 and 2004), which provides estimates of eddy dissipation rate (EDR, $\varepsilon^{1/3}$), an aircraft-independent atmospheric turbulence metric. This system reports turbulence measurements from

* *Corresponding author address:* John K. Williams, National Center for Atmospheric Research, P.O. Box 3000, Boulder, CO 80307; email: jkwillia@ucar.edu.

approximately one-minute intervals, including both the average and peak EDR encountered in the time since the previous report. The present study utilizes the peak EDR value because it supplies a better indication of hazard to the aircraft. In performing the comparisons presented below, the location of the aircraft corresponding to each EDR report was taken to be the midpoint between the report location and the location of the previous report. Since commercial aircraft typically fly at airspeeds near 250 m s^{-1}, these EDR measurement locations may be in error by 4 nmi (7.4 km) or more. Additionally, uncertainty in the location of the convection arises from the radar measurement, mosaicking and temporal delays inherent in the data collection and transmission processes. The spatial and temporal matching problem is even greater for pilot reports (PIREPs), which frequently involve significant uncertainty in the reported event's location and time (Schwartz 1996). Hence, the availability of the automated *in situ* EDR reports is essential to this study. Furthermore, unlike the limited data available from research flights, these reports provide turbulence measurements in conditions representative of those routinely encountered by commercial aircraft.

3.1 *Horizontal proximity based on NCWD*

The first proximity comparisons utilize the National Convective Weather Detection (NCWD) product, which is created and utilized as part of the NCW Forecast system. The NCWD product is described in Megenhardt et al. (2004). Briefly, the NCWD provides a 2-D mosaic of convective intensity on a 4-km grid that can be described using the six-level Video Integrator and Processor (VIP) scale. The detection product makes use of the WSR-88D (NEXRAD) Level III vertically integrated liquid (VIL) data via a mosaic supplied by UNISYS, and cloud-to-ground lightning data from the National Lightning Detection Network (NLDN). VIL data at locations having radar echo tops below 15,000 ft. are removed. The number of lightning strikes over the past 10 minutes within 8 km of a grid point are combined with the latest VIL mosaic to create the NCWD product, which is updated every 5 minutes.

The NCWD comparisons presented below are based on data collected between 9 August 2005 and 21 September 2005. For each *in situ* EDR report, a 2° x 2° area of the NCWD grid surrounding the point was retrieved. Within this area, the closest point (in great circle distance) was found which had NCWD-indicated convective intensity above a specified threshold. The plots presented in Figure 1 - Figure 5 show the relative frequency of four different levels of *in situ* turbulence as a function of distance from NCWD convection intensities corresponding to VIP levels 1-5, respectively. VIP level 1 corresponds to light precipitation, level 4 is heavy rain, and level 5 is explicitly referenced as an indication of intense convection in FAA AC 00-24. The levels of turbulence are light (EDR 0.1 – 0.2 $m^{2/3}$ s^{-1}), light to moderate (EDR 0.2 – 0.3 $m^{2/3}$ s^{-1}), moderate (EDR 0.3 – 0.4 $m^{2/3}$ s^{-1}), and moderate to severe (EDR 0.4 – 0.5 $m^{2/3}$ s^{-1}). The number of reports of higher EDRs was too small to obtain statistically significant results.

The relative frequencies of EDR reports at the various levels were calculated as a fraction of all reports having distances falling in each of a series of bins of width 4 nautical miles, or 7.408 km. To obtain error bar estimates, a binomial distribution was used. For a binomial distribution, the probability of x "successes" in n trials is given by the following formula, where p represents the probability of success in one trial:

$$P(x,p,n) = \frac{n!}{x!(n-x)!} p^x (1-p)^{n-x} \quad (1)$$

The standard deviation of x is

$$\sigma_x(p,n) = \sqrt{n\,p\,(1-p)} \quad (2)$$

Therefore, if $\hat{x}$ represents the empirical number of successes, and the empirical probability of success is

$$\hat{p} = \frac{\hat{x}}{n} \quad (3)$$

then the 95% confidence (two standard deviation) interval for x may be estimated as

$$x \in \hat{x} \pm 2\sqrt{n\,\hat{p}\,(1-\hat{p})} \quad (4)$$

It follows that, with 95% confidence,

$$p = \frac{x}{n} \in \hat{p} \pm 2\sqrt{\frac{\hat{p}\,(1-\hat{p})}{n}}\,. \quad (5)$$

In the present analysis, n represents the total number of turbulence reports in the distance bin and $\hat{x}$ is the number having the specified turbulence intensity level. The relative frequency is given by (3), with error bars determined via (5). However, it should be kept in mind that this error analysis only accounts for random sampling errors, and not for a possible lack of representativeness of the dataset. Thus, the error bars should be taken as suggestive but not precise.

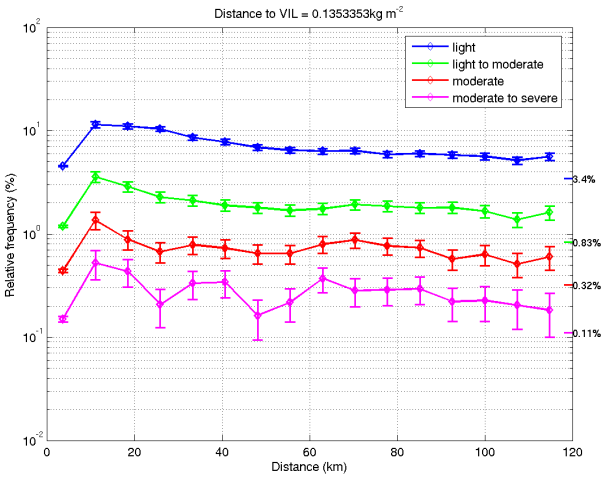

Figure 1: Relative frequencies of *in situ* light, light to moderate, moderate, and moderate to severe turbulence reports as a function of distance to NCWD convection intensity corresponding to VIP level 1 (light precipitation). The overall frequencies of the turbulence intensity levels in the entire *in situ* EDR dataset are indicated on the right side of the plot.

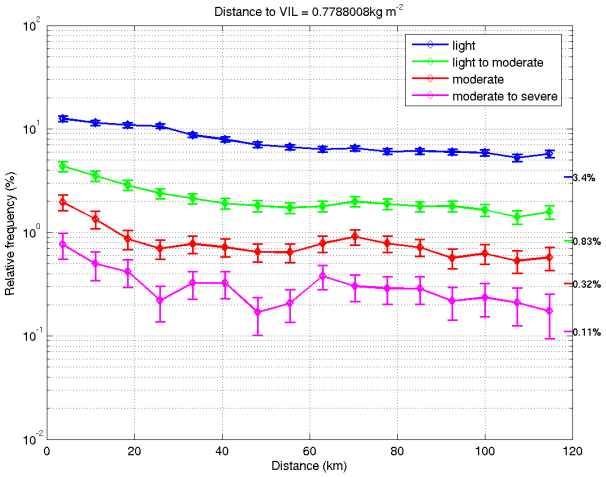

Figure 2: Same as Figure 1, but for VIP 2 (light to moderate rain).

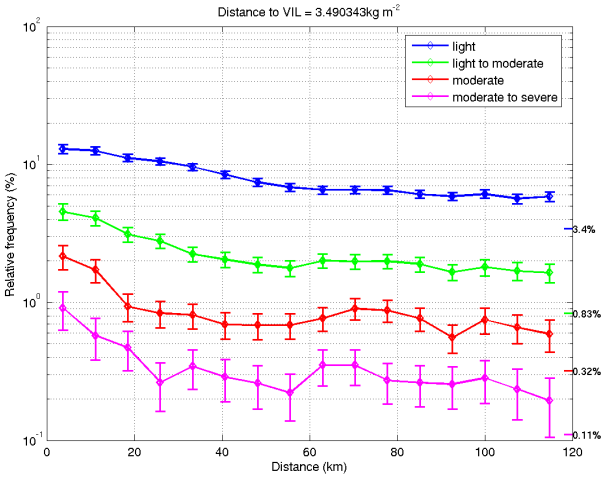

Figure 3: Same as Figure 1, but for VIP 3 (moderate to heavy rain).

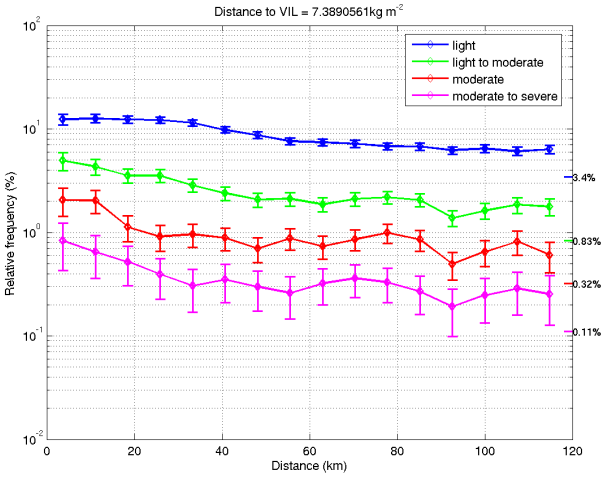

Figure 4: Same as Figure 1, but for VIP 4 (heavy rain).

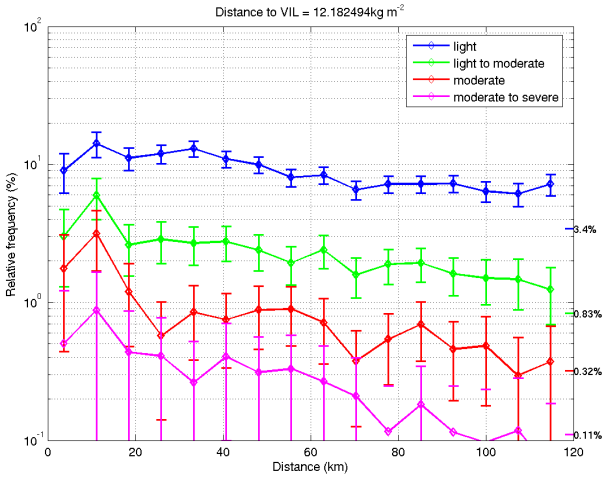

Figure 5: Same as Figure 1, but for VIP 5 (very heavy rain and possible hail).

3.2 *Horizontal proximity based on NTDA reflectivity*

In the summer of 2005, an operational demonstration of the NCAR Turbulence Detection Algorithm was performed (Yee et al. 2006, Sharman et al. 2006). In addition to EDR, a 3-D mosaic of radar reflectivity was produced for 16 NEXRADs in the upper Midwest, with horizontal spacing of 2 km and vertical levels at multiples of 3,000 ft. The comparisons with the reflectivity mosaic data shown below covered the period from 9 August 2005 to 28 September 2005. Since, unlike the NCWD, the NTDA reflectivity mosaic did not cover the entire conterminous United States, fewer convective cases were available for comparison. Only comparisons for reflectivity levels of 20, 30, and 40 dBZ are shown below; for higher reflectivity values there were to few data points to produce statistically meaningful results.

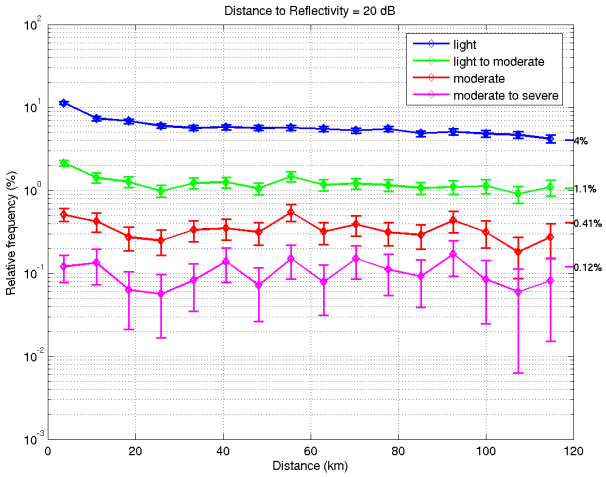

Figure 6: Same as Figure 1, but for NTDA reflectivity mosaic contour at 20 dBZ (light precipitation). The overall frequencies of the *in situ* turbulence intensity levels in are again indicated on the right side of the plot, but are slightly different for this dataset.

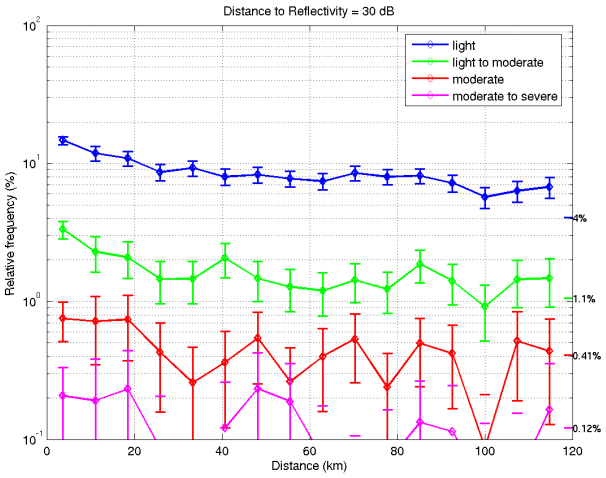

Figure 7: Same as Figure 6, but for NTDA reflectivity mosaic contour at 30 dBZ (light to moderate rain).

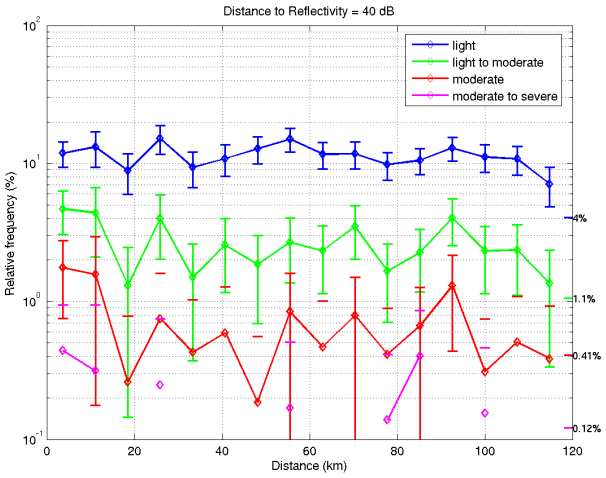

Figure 8: Same as Figure 6, but for NTDA reflectivity mosaic contour at 40 dBZ (moderate to heavy rain).

3.3 *Vertical proximity based on NTDA reflectivity*

A vertical comparison was also performed using the NTDA radar reflectivity mosaic. In performing this comparison, the vertical column of data which was closest to the *in situ* measurement point was identified, and the highest and lowest levels above the given reflectivity threshold were located. The vertical distance from the *in situ* point to the specified reflectivity was then calculated as the minimum to the top or bottom level, or reported as zero if the *in situ* altitude was between the top and bottom levels. If the column did not contain any values above the reflectivity threshold, it was ignored. It should be mentioned that, while in general it would be unwise to compare a point having uncertain position to a single grid column, the NTDA reflectivity grid is already significantly smoothed, ameliorating this complication. Unfortunately, even fewer cases were available for the vertical proximity comparison than for the horizontal, probably because commercial aircraft tend to avoid flying above or below cloud. Only comparisons for 20 and 30 dBZ thresholds are shown, and several points are missing from each due to the absence of any samples in the associated distance bin. Nevertheless, clear trends can still be seen.

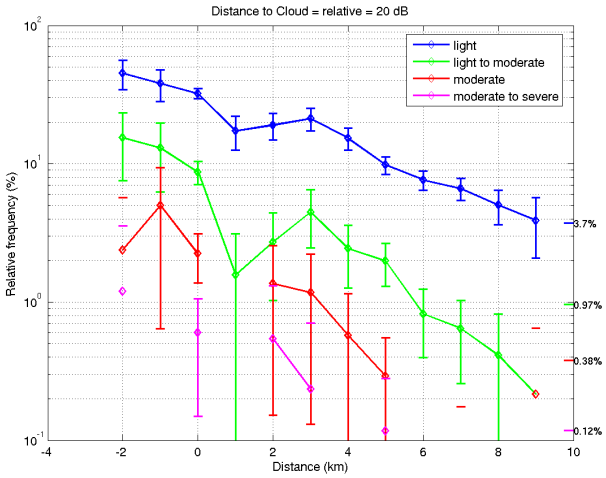

Figure 9: Same as Figure 6, but for vertical proximity to NTDA reflectivity mosaic of 20 dBZ (light precipitation).

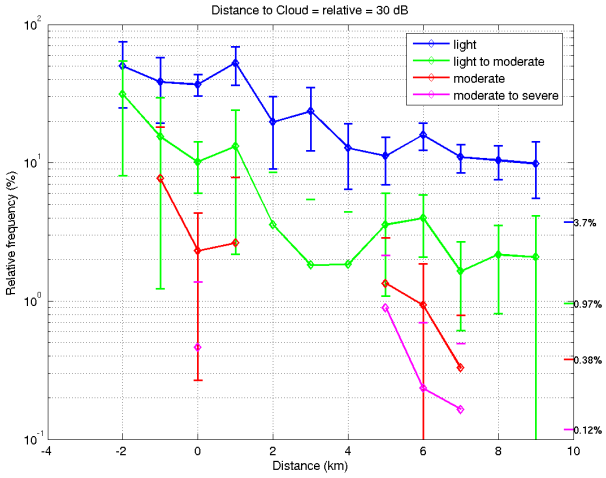

Figure 10: Same as Figure 9, but for vertical proximity to NTDA reflectivity mosaic of 30 dBZ (light to moderate rain).

4. CASE STUDIES

Another approach to assessing the current CIT avoidance guidelines is to perform case study analyses of a variety turbulent events. The chosen events should capture cases in which aircraft encountered moderate or greater turbulence both within and outside the area defined as hazardous to aviation by the CIT guidelines. The cases described here were chosen based on close proximity to a high reflectivity area and a peak *in situ* EDR reading of 0.35 $m^{2/3}$ s^{-1} or greater.

4.1 14 June 2004

The first case presented occurred on 14 June 2004 at 1210 UTC over central Iowa. The flight originated in Omaha, NE and was en-route to Chicago, IL (O'Hare) when the onboard *in situ* recording device measured a peak EDR value of 0.55 followed by several 0.25 and 0.15 readings (Figure 11). At the time of the encounter the aircraft was at flight level (FL)330 (or 33,000 ft for a standard atmosphere) and approaching a thunderstorm from the west. The movement of the convective complex was to the east. The 4 km IR GOES-12 satellite imagery from 1215 UTC (Figure 12) shows a well defined edge to the thunderstorm. Notice that the event (marked by the red cross) was on the very western boundary of the thunderstorm as defined by the satellite image. The satellite image nearest in time was approximately 5 min later than the actual turbulence event. Presumably the cloud edge 5 min prior to Fig. 2 would have been slightly further west according to the movement of the convective complex, which was eastward. When looking at the radar mosaic from the exact time of the turbulence encounter (Figure 13), however, the event appears to be about 20 km to the west of the boundary as defined by the edge of the radar echo.

The coldest cloud top temperatures, as measured by the IR GOES-12 satellite (Figure 12), in the most developed part of the convective cloud were around -45ºC. The closest complete upper air sounding to the event location was launched from Omaha, NE (about 125 miles from the turbulence encounter) at 12 UTC. According to that sounding, a temperature of -45ºC was measured around 10.8 km (just under 35,500 ft). At the time of the turbulent event the aircraft was at FL330 (which was below the highest cloud top further to the east), still ascending to its final cruising altitude of FL370. In order to find the true altitude of the aircraft the flight level was converted from standard to actual pressure level. It was found that the true aircraft altitude was about 700 ft above the standard atmospheric pressure level at 200 mb (i.e. when the aircraft was reporting a flight level of 37,000 ft it was actually flying at about 37,700 ft). Shortly after the turbulence encounter, while the aircraft was over the convective complex, it appears that they deviated slightly north around the highest portion of the cloud tops (which were around 35,500 ft), and were indeed flying above the cloud tops, in clear air. During this portion of the flight no significant turbulence was measured by the *in situ*.

Vertical wind shear and stability are two parameters that can play an important role in turbulence generation and maintenance. Together these two parameters make up the Richardson number (Ri) as the ratio of stability over shear squared. When Ri becomes small Kelvin-Helmholtz (KH) instabilities may develop which have been shown to produce turbulence, in some situations (e.g., Dutton and Panofsky 1970). Ri is given by:

$$Ri = N^2 / S_V^2 \tag{6}$$

where

$$N^2 = \frac{g}{\theta}\frac{\partial \theta}{\partial z} \text{ or } \frac{g}{\theta_e}\frac{\partial \theta_e}{\partial z} \tag{7}$$

and

$$S_V = \left|\frac{\partial \mathbf{v}}{\partial z}\right| \tag{8}$$

with θ potential temperature, θ_e equivalent potential temperature, g acceleration due to gravity, z the vertical direction, and $\boldsymbol{v}$ the horizontal wind vector with components u, v in the east-west and north-south directions, respectively.

The 1200 UTC analysis data from the Rapid Update Cycle (RUC; Benjamin et al. 2004) Numerical Weather Prediction (NWP) model was used to find the wind speed, along with calculated shear in the vertical at the exact location of the turbulence encounter. The Ri was also computed in the vertical and shown near the turbulence location. There is a spike in the shear value around 10 km near the altitude of the turbulence encounter (Figure 14). There is also a relative minimum in Ri at that same altitude (Figure 15). Both the high shear and low Ri values are indicative of the potential for turbulence at that location.

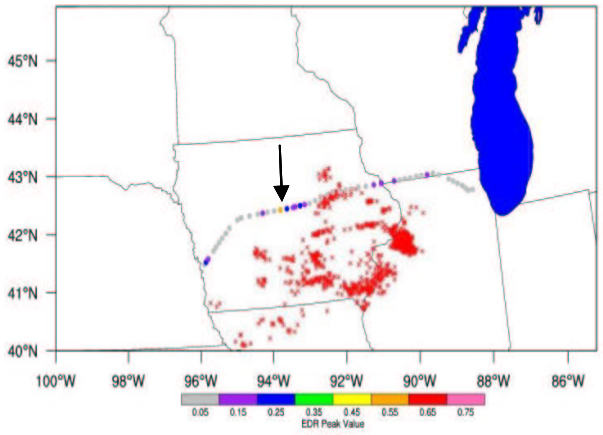

Figure 11: Aircraft flight track (flying from Omaha, NE to Chicago, IL) shown as peak EDR reports. Red asterisks reperesent cloud-to-ground lightning strikes which occurred between 1200-1230 UTC. The max peak EDR reading of 0.55 occurred at 1210 UTC.

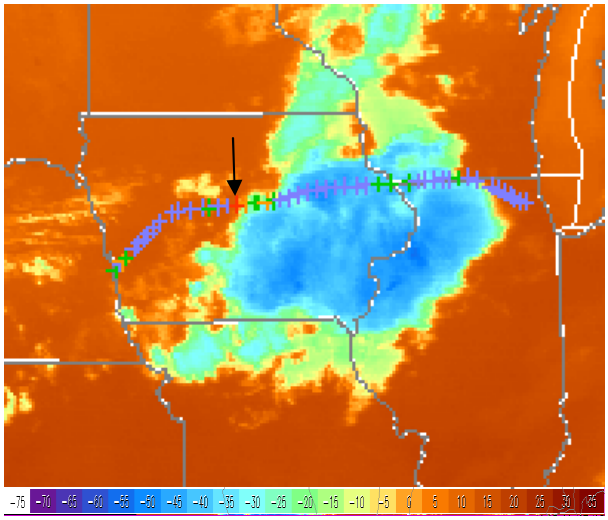

Figure 12: IR GOES-12 satellite image from 1215 UTC, 5 min after the turbulence event. The crosses denote the flight path with blue being peak EDR reading of 0.05, green 0.15, orange 0.25 and red 0.55.

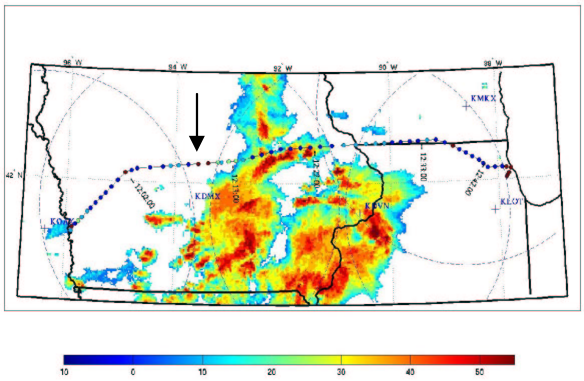

Figure 13: Radar mosaic data from 1210 UTC with the flight path and peak EDR measurements overlaid. The color scale at the bottom applies to the radar reflectivity values as well as the peak EDR values multiplied by 100.

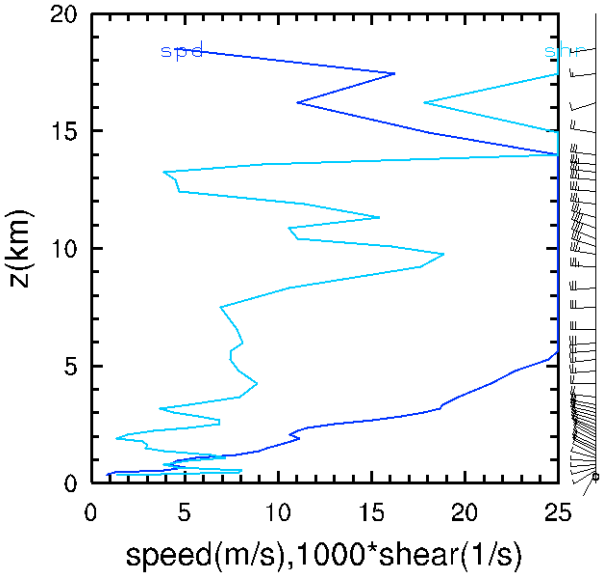

Figure 14: Wind speed and computed wind shear from the 12 UTC initialization of the RUC NWP model at the location of the turbulence encounter.

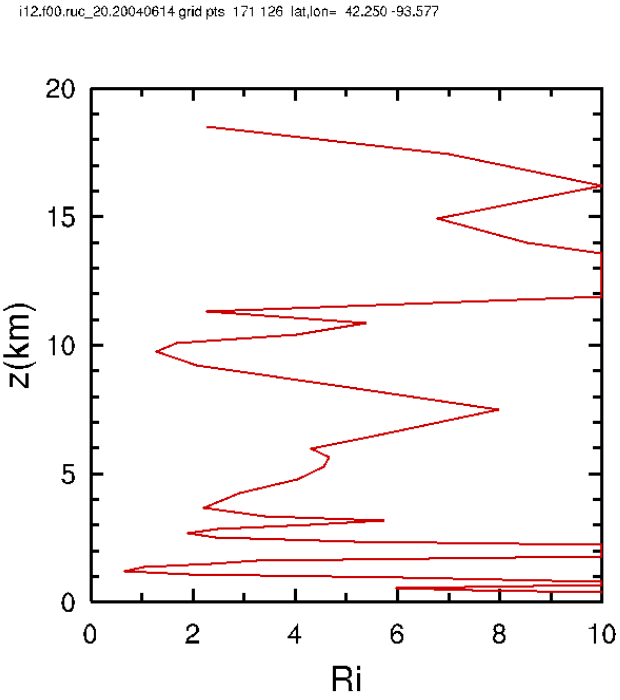

Figure 15: Computed Richardson number (Ri) from the 12 UTC initialization of the RUC NWP model at the location of the turbulence encounter.

4.2 18 May 2004

Another case investigated occurred on 18 May 2004 over north-central Ohio at 1811 UTC. The flight was in cruise from Pittsburgh, PA to Chicago (O'Hare), IL and had to navigate through several "popcorn" type thunderstorm cells. The onboard *in situ* measured one reading of 0.35, with a few other lighter bumps of 0.15 along the flight path (Figure 16). At the time of the maximum *in situ* reading the aircraft was in cruise at FL350. The cells were all moving in an east-northeast direction. At the time of the encounter, the aircraft appeared to be about 40 km from the nearest thunderstorm cell (which was to the south), however, there were also a few smaller cells directly to the north and east about 60 km away (Figure 17). The IR GOES-12 satellite image also shows the spotty nature of the thunderstorms with definite clear air surrounding them (Figure 18). The strongest *in situ* measurement of 0.35 (marked with the red cross) appears to be definitely out of cloud at the time of the occurrence. The difficulty with this case is in understanding all of the forcing mechanisms occurring around each individual thunderstorm cell, as well as the system as a whole, in order to attribute the turbulence encounter to a specific source.

The calculated shear (Figure 19) and Ri (Figure 20) at the specific location of the turbulence encounter are again shown for this event. The shear is moderately high at the location of the ecounter, however, the Ri is also fairly high. The high Ri values with high shear implies that the area is convectively stable and there are likely other mechanisms contributing to this encounter.

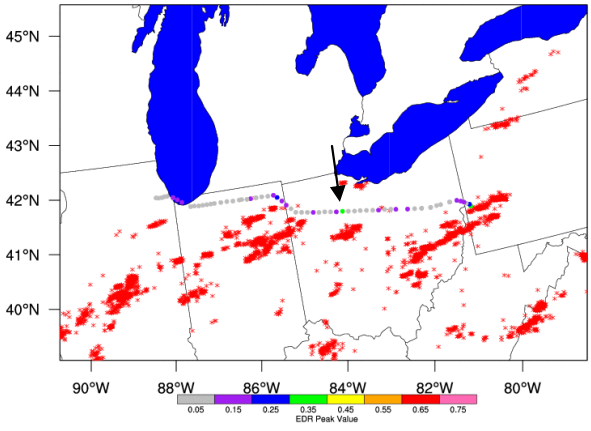

Figure 16: Aircraft flight track (flight from Pittsburgh, PA to Chicago, IL) shown as peak EDR reports. Red asterisks represent cloud-to-ground lightning strikes which occurred between 1800-1830 UTC. The max peak EDR reading of 0.35 occurred at 1811 UTC.

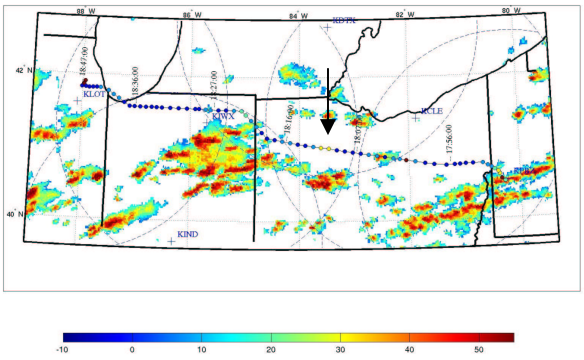

Figure 17: Radar mosaic data from 1810 UTC with the flight path and peak EDR measurements overlaid. The color scale at the bottom applies to the radar reflectivity values as well as the peak EDR values multiplied by 100.

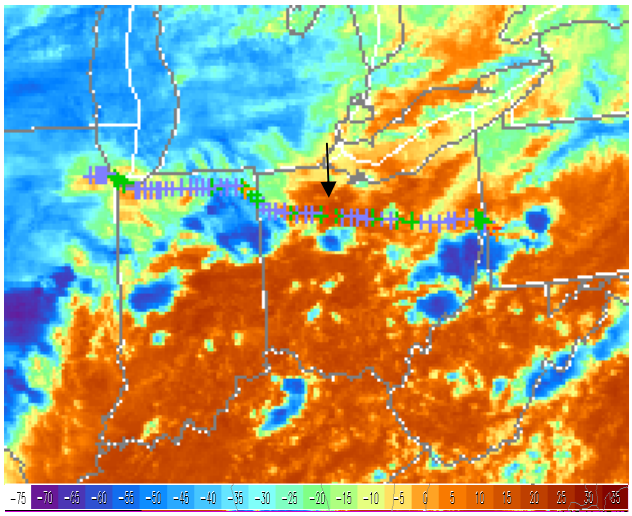

Figure 18: IR GOES-12 satellite image from 1815 UTC. The red cross marks the location of the peak EDR reading of 0.35, which occurred 4 min prior to this image at 1811 UTC.

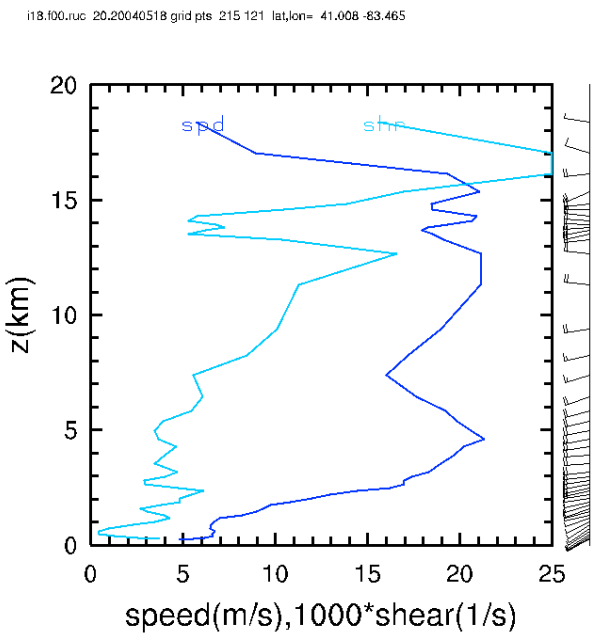

Figure 19: Wind speed and computed wind shear from the 18 UTC initialization of the RUC NWP model at the location of the turbulence encounter.

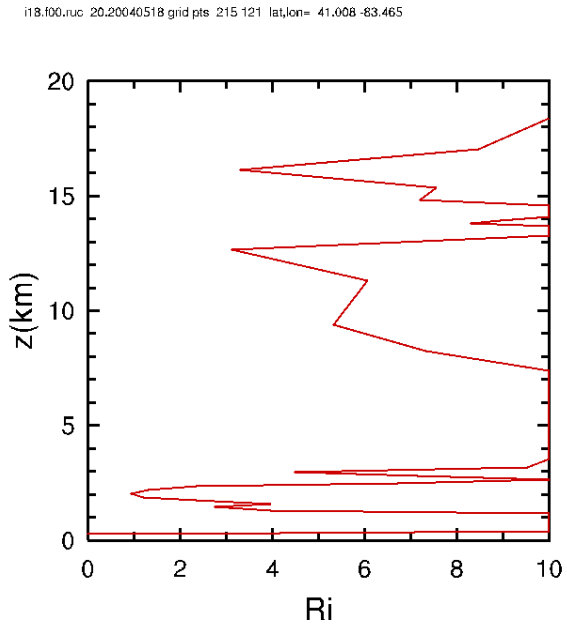

Figure 20: Computed Richardson number (Ri) from the 18 UTC initialization of the RUC NWP model at the location of the turbulence encounter.

It well known that shear and stability are very important parameters in identifying areas of potential turbulence in general. This was also evident in the case studies. By coupling these types of indicators with information about areas of high reflectivity on a season-wide time scale via statistical comparisons like those presented in the previous section, it is hoped that more information about CIT will be obtained and new avoidance guidelines may emerge.

These empirical case studies underline the need for a better understanding of the turbulence generation processes in the clear air in the proximity of thunderstorms. Hydrostatic mesoscale models such as the RUC clearly do not have a sufficient resolution or dynamical treatment of the processes that might be generating turbulence at the scales important for aircraft. High resolution simulations using a nonhydrostatic model are for an adequate representation of the cloud, its environment, and its casual relation to turbulence. One such study was that of Lane et al. (2003) which studied in detail a severe turbulence encounter above isolated deep convection. In that study it was found that gravity waves of wavelength about 2 km were produced above the cloud as the rapidly growing cloud penetrated the lower stratosphere. The gravity waves propagated vertically upward several km above the stratosphere, and "broke" to produce turbulence in the clear air above the cloud, in this case near the gravity wave's critical level. If this is a general result, since the critical level would be a function of the vertical distribution of the wind and stability, as well as the cloud propagation speed, the turbulence generation process associated with convection may be indeed very complex. Similar studies need to be performed to better understand how these and possibly other environmental parameters may relate to CIT in order to produce useful diagnostics for thunderstorm avoidance guidelines.

5. CONCLUSION

The current FAA guidelines for flying near thunderstorms include several restrictions based on the need to avoid out-of-cloud CIT. Because these guidelines have a potentially significant impact on both aviation safety and on the efficiency of flight operations during widespread convection, a study is underway to attempt to evaluate the guidelines and, if possible, either confirm that they are appropriate or suggest principled alternatives.

The relatively new availability of *in situ* turbulence measurements from the FAA's automated EDR reporting system made the statistical and case studies presented in this paper possible. The statistical analyses related turbulence measurements to their proximity to convection, as indicated by the NCWD convective intensity product and the NTDA 3-D reflecitivity. Results of these analyses generally supported the current CIT avoidance guidelines, as all levels of turbulence were seen to diminish as the distance from convection grew, with a significant diminution of higher levels of turbulence having occurred by a distance of 20 nautical miles (37 km). Interestingly, light turbulence appeared to take longer to disappear with distance from convection, and reports of turbulence at all magnitudes remained somewhat elevated for large distances. Additionally, the vertical

proximity data underscore the danger of flying under cloud, where a high incidence of turbulence reports was observed. More data is needed to evaluate these phenomena more accurately, and for the reflectivity analysis discrimination between convective and stratiform precipitation cases would be useful. A more comprehensive analysis is planned that will utilize additional morphological features (e.g., to identify anvils) and storm growth rate data. Furthermore, as the case studies suggest, an examination of additional environmental data, such as may be obtained from the RUC model, may also be profitable. Finally, additional numerical simulation studies will be helpful in further understanding the mechanisms for CIT generation.

In addition to a possible update of the FAA's CIT avoidance guidelines, it is hoped that insights gained from this work may lead to the development of diagnostics for CIT that could be implemented in an automated system. These would supplement the upper-level turbulence forecasts currently supplied by GTG on the National Weather Service Aviation Weather Center's Aviation Digital Data Service (ADDS). Eventually, these diagnostics may be combined with satellite, *in situ*, and numerical weather prediction model data to identify and forecast regions of hazardous convectively-induced turbulence. The resulting rapid-update turbulence "nowcast" capability could significantly improve aviation safety, passenger confidence, and air traffic flow during convective events.

6. ACKNOWLEDGEMENTS

The authors wish to express our appreciation to the Turbulence PDT's en-route turbulence project, including Larry Cornman, Martha Limber, and Sue Dettling, for supplying the *in situ* EDR data used in this study. And many thanks to Dan Megenhardt and the Convective Weather PDT for providing and explaining the NCWD product.

This research is in response to requirements and funding by the Federal Aviation Administration (FAA). The views expressed are those of the authors and do not necessarily represent the official policy or position of the FAA.

7. REFERENCES

Benjamin, S. G., G. A. Grell, J. M. Brown, T. G. Sminova, and R. Bleck, 2004: Mesoscale weather prediction with the RUC hybrid isentropic-terrain-following coordinate model. *Mon. Wea. Rev*., **132**, 473-494.

Cornman, L. B. and B. Carmichael, 1993: Varied research efforts are under way to find means of avoiding air turbulence. *ICAO Journal*, 48, 10-15.

Cornman, L. B., C. S. Morse, and G. Cunning, 1995: Real-time estimation of atmospheric turbulence severity from in-situ aircraft measurements, *Journal of Aircraft*, 32, 171-177.

Cornman, L. B., G. Meymaris and M. Limber, 2004: An update on the FAA Aviation Weather Research Program's *in situ* turbulence measurement and reporting system. *11th AMS Conference on Aviation, Range, and Aerospace Meteorology*.

Dutton, J., and H. A. Panofsky, 1970: Clear air turblulence: A mystery may be unfolding. *Science*, **167**, 937-944.

Kaplan, M. L, A. W. Huffman, K. M. Lux, J. J. Charney, A. J. Riordan, and Y.-L. Lin, 2005: Characterizing the severe turbulence environments associated with commercial aviation accidents. Part 1: A 44-case study synoptic observational analyses. *Meteor. Atmos. Phys.*, **88**, 129-153.

Lane, T. P., R. D. Sharman, T. L. Clark, and H.-M. Hsu, 2003: An investigation of turbulence generation mechanisms above deep convection. *J. Atmos. Sci.*, **60**, 1297-1321.

Megenhardt, D. L., C. Mueller, S. Trier, D. Ahijevych, and N. Rehak, 2004: NCWF-2 Probabilistic Forecasts. *11th AMS Conference on Aviation, Range, and Aerospace Meteorology*, 5.2.

Schwartz, B., 1996: The quantitative use of PIREPs in developing aviation weather guidance products. *Wea. Forecasting*, **11**, 372-384.

Sharman, R., C. Tebaldi, J. Wolff and G. Wiener, 2002: Results from the NCAR Integrated Turbulence Forecasting Algorithm (ITFA) for predicting upper level clear-air turbulence. *10th AMS Conference on Aviation, Range, and Aerospace Meteorology*, 351-354.

Sharman, R. D., L. Cornman, J. K. Williams, S. E. Koch, and W. R. Moninger, 2006: The AWRP Turbulence PDT. *12th AMS Conference on Aviation, Range, and Aerospace Meteorology*, 3.3.

Yee, J., J. K. Williams, S. G. Carson and J. Craig, 2006: Turbulence Remote Sensing Operational Demonstration System. *22nd International Conference on Interactive Information Processing Systems for Meteorology, Oceanography, and Hydrology*, P1.2.